A&A 442, 1107–1120 (2005)
DOI: 10.1051/0004-6361:20041571

Astronomy & Astrophysics

The chemistry of C_2 and C_3 in the coma of Comet C/1995 O1 (Hale-Bopp) at heliocentric distances $r_h \geq 2.9$ AU⋆,⋆⋆

J. Helbert[1], H. Rauer[2], D. C. Boice[3], and W. F. Huebner[3]

[1] Institute of Planetary Research, DLR, Rutherfordstr. 2, 12489 Berlin, Germany
e-mail: joern.helbert@dlr.de
[2] Institute of Planetary Exploration, DLR, Rutherfordstr. 2, 12489 Berlin, Germany
[3] Southwest Research Institute, PO Drawer 28510, San Antonio, TX 78228-0510, USA

Received 1 July 2004 / Accepted 21 April 2005

ABSTRACT

The extraordinary activity of comet C/1995 O1 (Hale-Bopp) made it possible to observe the emission bands of the radicals C_2 and C_3 in the optical wavelengths range at heliocentric distances larger than 3 AU. Based on these observations, we perform an analysis of the formation of C_2 and C_3 in a comet coma at large heliocentric distances. We present the most complete chemical reaction network used until today, computing the formation of C_2 and C_3 from C_2H_2, C_2H_6, and C_3H_4 as their parent molecules. The required photodissociation rates of C_3H_2 and C_3 had to be derived based on the observations. The spatial distributions of C_2 and C_3 calculated with the chemical model show good agreement with the observations over the whole range of heliocentric distances covered in this work. Based on the production rates for C_2H_2, C_2H_6, and C_3H_4, abundance ratios are obtained for heliocentric distances $r_h \geq 3$ AU. In comet Hale-Bopp, C_2H_2 and C_2H_6 were measured directly by infrared observations only at heliocentric distance $r_h \leq 3$ AU (Dello Russo et al. 2001). The model presented here greatly extends the heliocentric distance range over which hydrocarbons can be studied in the coma of comet Hale-Bopp. We discuss possible indications of these abundance ratios for the formation region of comet Hale-Bopp.

Key words. comets: general – comets: individual: C/1995 O1 (Hale-Bopp) – planets and satellites: formation – interplanetary medium

1. Introduction

C_2 was the first radical identified by spectroscopic measurements in the coma of a comet (Donati 1864; Huggins 1867). Jackson (1976) was one of the first to propose acetylene C_2H_2 and ethane C_2H_6 as likely parent molecules for C_2. Subsequent modeling by numerous authors, e.g. Cochran (1985) and Yamamoto (1981) supported this idea and established a link between C_2 and C_2H_2 assuming only photodissociation reactions. However, these early model attempts did not entirely solve this problem and several uncertainties remained. It took more than a century from the first detection of C_2 until the proposed parent molecules, C_2H_2 and C_2H_6, have been observed for the first time in the comae of the comets Hale-Bopp and Hyakutake (Brooke et al. 1996; Tokunaga et al. 1996; Mumma et al. 1996). The situation for C_3 was even worse. Although Donati (1864) and Huggins (1867) had reported emissions at 4050 Å, it took nearly 80 years until Douglas (1951) identified these correctly as C_3 emission bands. Swings (1965) proposed C_4H_2 as a parent molecule for C_3. Stief et al. (1972) showed that this is unlikely based on the reaction efficiencies and proposed formation of C_3 by a single photodissociation step from propyne CH_3C_2H (often also called methylacetylene) instead. Jackson (1976) discussed a two-step formation with C_3H_2 as the intermediate product. An analysis of Haser parent scale lengths for C_3 by Yamamoto (1981) and Krasnopolsky (1991) confirmed that formation of C_3 in a single dissociation step is unlikely.

With the current work, we show a reaction network which links C_2 with both proposed parent molecules considering photodissociation and electron impact dissociation, as has already been proposed by Boice et al. (1998). At the same time, the network is capable of explaining the formation of C_3 from C_3H_4 in both its main isomeric forms (allene and propyne) assuming multi-step reactions and competing reaction pathways. Sometimes a third isomer of C_3H_4 cyclopropene is discussed. This isomer is an excited state of propene. Due to the inherent ring strain, this cyclic isomer undergoes readily ring-opening, forming allene (Faber et al. 2001). Therefore we do not consider it as a main parent, but instead as a contribution to allene. In the past, observations of C_2 and C_3 have received limited interest, because of the unclear link to the parent species in the nucleus. With our reaction network, this link is established and

⋆ Based on observations collected at the European Southern Observatory, Chile.
⋆⋆ Table 4 is only available in electronic form at http://www.edpsciences.org

Table 1. Subset of the data from Rauer et al. (2003) used for analysis with the ComChem model. The first column gives the date of the observation, r_h (negative for pre-perihelion) and Δ are the heliocentric and geocentric distance of the comet, the fourth column gives the telescope and instrument used, the fifth column denotes how many spectra have been averaged in the observing run, the sixth column shows the resulting total integration time, $\Delta\rho$ is the spatial resolution of the profiles and the last column lists comments on the observations.

Date	r_h [AU]	Δ [AU]	Telescope/ Instr.	Number of spectra averaged	Total int. time [s]	$\Delta\rho$ 10^3[km]	Comment
17.8.1996	–3.39	2.8	Danish 1.5/DFOSC	2	1800	7.86	C_3 contaminated
2.10.1996	–2.86	3.0	Danish 1.5/DFOSC	2	1800	8.09	
23.11.1997	3.51	3.4	ESO 1.5/B&C	4	4800	18.8	not photometric
6.12.1997	3.66	3.5	Danish 1.5/DFOSC	6	5400	10.3	C_3 contaminated
19.12.1997	3.78	3.6	ESO 1.5/B&C	3	3600	21.6	
20.1.1998	4.13	4.0	ESO 1.5/B&C	4	3900	23.7	
21.1.1998	4.14	4.0	Danish 1.5/DFOSC	4	3900	11.7	C_3 contaminated
21.3.1998	4.74	4.8	ESO 1.5/B&C	3	2700	25.6	

observations of C_2 and C_3 in the optical wavelengths range can be used to derive information about the nucleus, its composition and history.

2. The coma chemistry model

The ComChem model has been developed mainly by Huebner and Boice over more than two decades (Giguere & Huebner 1978; Boice et al. 1986, 1998; Huebner et al. 1987; Schmidt et al. 1988). The model is a multifluid, hydrodynamic model for the gas flow in the coma of a comet. It assumes insolation angle-dependent sublimation of ice on the sunlit hemisphere and, after pressure equalization above the Knudsen layer, isotropic radial outflow and expansion of the coma gas. Using these assumptions, a 1-D neutral coma is modeled with a detailed treatment of the photo and gas-phase chemistry. A special focus is placed on the self-consistent description of dynamics and chemistry in the coma. Gas dynamics and chemical reactions are coupled processes, therefore, they need to be modeled together. The model allows for a study of various coma properties, e.g., spatial distributions of gas-phase species and the velocity and temperature profiles and their changes with heliocentric distance. Dust entrainment is not considered in this work, but would be part of a full model. For a detailed description of the model see, for example, Huebner et al. (1987) and Schmidt et al. (1988).

3. Coma profiles used for the analysis

Data from the Hale-Bopp optical monitoring program have been used for this analysis. Within this program, comet Hale-Bopp has been observed with optical long-slit spectroscopy at the European Southern Observatory (ESO) in Chile and the Observatoire Haute-de-Provence in France (Rauer et al. 1997, 2003). Observations before perihelion cover the heliocentric distance range from 4.6−2.8 AU, while the observations after perihelion cover the range from 2.9−12.8 AU. For detailed information on the observations and the data reduction see Rauer et al. (2003). Emission bands of the CN, C_3, C_2, and NH_2 radicals have been followed in this observing campaign. While all emission bands appeared in the first observations at 4.6 AU pre-perihelion (Rauer et al. 1997), emissions of NH_2 could be followed up to 4.7 AU post-perihelion, C_2 up to 5.0 AU, and C_3 and CN up to 7.0 AU and 9.8 AU, respectively (Rauer et al. 2003).

For the analysis using the ComChem model, only a subset of the observations obtained in the longterm monitoring program is used. The criteria are the quality of the measurement of the C_2 and the C_3 spatial column density profiles. The radial extension of the profile and the S/N ratio over the whole radial profile should allow a clear identification of the shape of the profile. For the set of observations used for this study, this means a minimal projected radial extension of 2×10^5 km. Table 1 summarizes the observations used. A mean profile has been derived for each night by averaging all observations of the same night. The number of spectra averaged and the resulting total integration time is given in Table 1. The observations obtained at the Danish telescope suffer from light contamination caused by internal reflexions in the spectrograph. Unfortunately, this effect is worst at the position of the C_3 emission. For this reason, the C_3 profiles for the nights 17.8.1996, 6.12.1997, and 21.1.1998 can be used only inside 2×10^5 km of the projected nucleocentric distance. The observations obtained at larger heliocentric distances pre-perihelion are not included in this study for the same reason. The night of 23.11.1997 was not photometric and has only been used to derive reaction rates for the dissociation of C_3H_2 and C_3 from the profile shape.

4. The chemistry of possible C_2 and C_3 parents

The chemistry of possible C_2 and C_3 parents has been discussed by numerous authors. We will not reiterate all discussions in this paper. Instead, we briefly describe the chemistry used for our reaction network and highlight the differences of our approach to earlier work. While the whole reaction network used for the ComChem model in this study consists of more than 1000 reactions, only a subset of these play a significant role in the formation of the C_2 and C_3 radical. Approximately 200 reactions are related to the chemistry discussed here, a list is given in Helbert (2003). As will be discussed later, out of

these reactions approximately 20 dominate the formation of C_2 or C_3.

4.1. C_2H_6 chemistry

The photodissociation of ethane (C_2H_6) was studied by Calvert & Pitts (1966). The main products of the photolysis are C_2H_4 and CH_4. Unfortunately, the exact branching ratios are still unknown. They seem however to depend on the wavelength of the irradiating photon. While the first process is dominant only at 1236 Å, dissociation to CH_4 becomes increasingly important at large wavelengths.

$$\begin{aligned} C_2H_6 &\xrightarrow{h\nu} C_2H_4 + H_2 \\ &\xrightarrow{h\nu} C_2H_4 + 2\,H \\ &\xrightarrow{h\nu} CH_4 + CH_2 \\ &\xrightarrow{h\nu} 2\,CH_3 \\ &\xrightarrow{h\nu} C_2H_5 + H \end{aligned}$$

For reactions described in this paper, $\xrightarrow{h\nu}$ is used as a short notation for $+\,h\nu \longrightarrow$ and the asterisk marks an excited state.

The dissociation to C_2H_4, CH_2, and C_2H_5 are almost equally important. C_2H_6 dissociated to CH_2 and CH_4 is not contributing to the formation of C_2. The dissociation into these two products removes one third of the available C_2H_6 from the C_2 production. The dissociation product C_2H_4 has three main dissociation channels, where the dissociation to CH_2 is the main channel. Overall more C_2H_6 goes into the formation of CH_2 than into the formation of C_2H_2 which forms C_2. The C_2H_5 produced in the last reaction dissociates almost immediately to C_2H_2. For this reason, some authors do not even list this reaction (for example Lias et al. (1970) or Moses (2000, pers. comm.)). For completeness the intermediate product is included in this reaction network.

The photodissociation rate coefficients have been obtained mainly from Huebner et al. (1992). While the cross section for wavelengths below 250 Å is derived from the atomic cross sections of C and H, there are measurements for the cross sections from 354−1127 Å, from 1160 to 1200 Å, from 1200 to 1380 Å and from 1380 to 1600 Å (see Huebner et al. 1992, and references therein). Branching ratios leading to dissociation and ionization have been measured by Lias et al. (1970) at 1055, 1236 and 1470 Å. The photodissociation rate coefficients derived by Huebner et al. (1992) are in good agreement with recent data by Moses (2000, pers. comm.).

Little is known about the electron impact dissociation of C_2H_6. There are no reaction coefficients available, neither theoretical nor measured. Even the reaction pathways are unknown. One might assume that the electron impact dissociation of C_2H_6 will form similar products as the photodissociation reactions. Currently electron impact dissociation reactions of C_2H_6 are not included in the reaction network. This will be changed as soon as measurements become available. However, as will be shown later, C_2H_6 is not the main source of C_2. This result will hold true for a reaction network including electron impact dissociation of C_2H_6, unless these reactions are more effective than the photodissociation reactions by orders of magnitudes.

4.2. C_2H_2 chemistry

The photodissociation of C_2H_2 was studied by a number of authors, for example, Jackson (1976) and Jackson et al. (1996).

The main proposed sequence for dissociation of C_2H_2 is

$$\begin{aligned} C_2H_2 &\xrightarrow{h\nu} C_2H + H \\ C_2H &\xrightarrow{h\nu} C_2 + H \\ C_2 &\xrightarrow{h\nu} C_2^+ + e \end{aligned}$$

While this is the main photolytic channel for the production and destruction of the C_2 radical by C_2H_2, there is a second production channel by direct photodissociation of C_2H_2

$$C_2H_2 \xrightarrow{h\nu} C_2 + H_2$$

However, this reaction has a very low efficiency at a wavelength of 1930 Å based on Wodtke & Lee (1985). Integrated over the whole solar spectrum, this reaction is about one order of magnitude less important than the dissociation to C_2H (see Huebner et al. 1992).

In addition to ionization of C_2, the photodissociation of C_2 is the second channel for the destruction of this radical. In general, it is difficult to measure the photoabsorption cross sections of small radicals. Pouilly et al. (1983) have studied the photodissociation in the range from 918−1210 Å. Based on their results and the values for atomic carbon, Huebner et al. (1992) calculated the reaction rates.

The rate coefficients by Huebner et al. (1992) for the C_2H_2 photochemistry are in good agreement with recent data by Moses (2000, pers. comm.). For C_2H_2, Wu (2000, pers. comm.) has provided recent preliminary laboratory measurements of absorption cross sections at low temperatures. A comparison of the resulting dissociation rate coefficients showed only differences of less than a factor of two compared to the values obtained by Moses (2000, pers. comm.) and Huebner et al. (1992). For consistency, the values by Huebner et al. (1992) have been used for the C_2H_2 photodissociation. Once the complete measurements by Wu (2000, pers. comm.) are available these values can be updated.

For C_2H_2 we have also included electron impact dissociation reactions. The electron impact dissociation of C_2H_2 was studied in the laboratory by Pang et al. (1987).

There are two branches for the electron impact dissociation of C_2H_2.

$$\begin{aligned} R_1{:}\quad & C_2H_2 + e \longrightarrow C_2H + H \\ R_2{:}\quad & C_2H_2 + e \longrightarrow C_2 + H_2 \end{aligned}$$

Based on cross sections determined from the laboratory measurements and theoretical studies by Keady (see Boice et al. (1986) and Schmidt et al. (1988) and references therein) the temperature dependent cross sections given in Table 2 can be determined. Here k is the Arrhenius coefficient.

Table 2. Reaction rate coefficients for reaction R_1 and R_2 estimated by Boice et al. (1986).

T[K]	$k(R_1)$ [cm^3/s]	$k(R_2)$ [cm^3/s]
10 000	1.37×10^{-11}	9.32×10^{-12}
15 000	1.15×10^{-10}	2.13×10^{-10}
20 000	3.35×10^{-10}	1.01×10^{-9}
25 000	6.32×10^{-10}	2.57×10^{-9}
30 000	9.55×10^{-10}	4.77×10^{-9}

4.3. HC_3N as a possible additional parent molecule of C_2

We have also considered whether cyanoacetylene (HC_3N), would be another possible parent for C_2. As shown by Halpern et al. (1988), there are two possible dissociation reactions

$$\begin{aligned} HC_3N &\xrightarrow{h\nu} C_2H + CN \\ &\xrightarrow{h\nu} H + C_3N \end{aligned}$$

The second reaction is immediately followed by

$$C_3N \xrightarrow{h\nu} C_2 + CN$$

The dissociation of HC_3N via C_3N is the main channel as has been shown by Job & King (1966), Seki (1985), and Halpern et al. (1988).

Therefore, HC_3N is a parent of C_2 as well as a parent of CN. If significant amounts of C_2 are formed from HC_3N, this would imply also a significant production of CN. This is in contradiction to the findings by Rauer et al. (2003), who have shown that the CN production rate of comet Hale-Bopp can be explained by HCN as the dominant parent molecule for heliocentric distances larger than ≈3 AU. The abundance ratio of HC_3N relative to H_2O as measured by Bockelée-Morvan et al. (2000) was 0.02%, compared to 0.1% for C_2H_2 and 0.3% for C_2H_6 (Dello Russo et al. 2001). Therefore the contribution to the C_2 formation is within the error of the production rates derived in this model. We have not included HC_3N as a C_2 parent for these reasons.

4.4. Chemistry of the C_3 parent molecules

Stief et al. (1972) examined various potential parents, and proposed propyne (CH_3C_2H) as a plausible candidate. According to their work C_3 is formed via

$$CH_3C_2H + \xrightarrow{h\nu} C_3 + 2H_2$$

This would mean C_3 is formed in a single-step process. This is in contradiction to the results by Yamamoto (1981) and Krasnopolsky (1991) who indicate formation as a second-generation radical.

Jackson (1976) proposed the following two-step mechanism

$$\begin{aligned} CH_3C_2H &\xrightarrow{h\nu} C_3H_2 + H_2 \\ C_3H_2 &\xrightarrow{h\nu} C_3 + H_2 \end{aligned}$$

While most of the early work focused on propyne, there are two isomers of C_3H_4, allene (H_2CCCH_2), propyne (CH_3C_2H), and an an excited cyclic state of propene cyclopropene. As has been discussed already cyclopropene readily forms allene. Therefore we consider in this work only the two linear isomers as possible grandparents of C_3.

For the photodissociation of propyne at 1930 Å, Mebel et al. (1998) predicted that it occurs via a fast pathway including internal excitation and a slow pathway including internal isomerization into allene. In the fast pathway, propyne is excited and quickly eliminates the acetylenic hydrogen. This is followed by a dissociation to H_3CCC+H. The slow pathway includes the internal conversion into the vibrationally excited ground electronic state. The vibrationally excited propyne then dissociates to produce either H_2CCCH+H or HCCCH+H_2, or isomerizes to allene, which, in turn, dissociates to H_2CCC+H_2. The HCCCH produced from propyne can have sufficiently high internal energy to rearrange to H_2CCC.

The most likely mechanism for the photodissociation of allene at 1930 Å is to produce C_3H_2+H_2 via a vibrationally excited state of allene. It can also produce C_3H_3+H. The branching ratio was already determined by Jackson et al. (1991) experimentally to be 0.19 for the first and 0.81 for the latter reaction. The atomic hydrogen production channel dominates over the molecular hydrogen channel.

In both cases, the formation of C_3+H_2 from propyne and allene goes via the same intermediate. This is in agreement with the fact that the same rotational distribution of the C_3 products is observed in the laboratory. Unfortunately, this excludes the possibility to deduce the C_3 parent isomer from the observed C_3 excitation spectrum.

Both scenarios can be summarized as

Propyne:

$$\begin{aligned} &H_3CCCH \xrightarrow{h\nu} H_3CCCH^* \longrightarrow HCCCH^* + H_2 \\ &\quad \longrightarrow H_2CCC + H_2 \xrightarrow{h\nu} C_3 + 2H_2 \\ &H_3CCCH \xrightarrow{h\nu} H_3CCCH^* \longrightarrow H_2CCCH + H \\ &\quad \longrightarrow H_2CCC + 2\,H \xrightarrow{h\nu} C_3 + H_2 + 2\,H \\ &H_3CCCH \xrightarrow{h\nu} H_2CCCH_2 \xrightarrow{h\nu} H_2CCC + H_2 \\ &\quad \xrightarrow{h\nu} C_3 + 2H_2 \end{aligned}$$

Allene:

$$\begin{aligned} &H_2CCCH_2 \xrightarrow{h\nu} H_2CCC + H_2 \xrightarrow{h\nu} C_3 + 2H_2 \\ &H_2CCCH_2 \xrightarrow{h\nu} H_2CCCH + H \\ &\quad \xrightarrow{h\nu} H_2CCC + 2H \xrightarrow{h\nu} C_3 + H_2 + 2H \end{aligned}$$

Within these reaction schemes, only a few cross sections are available. For the dissociation of allene, there are measurements by Sutcliffe & Walsh (1952), Rabalais et al. (1971), and Fuke & Schnepp (1979). For the dissociation of propyne (CH_3C_2H) also known as methylacetylene, there are some measurements available by Fahr & Nayak (1996), Stief et al. (1971), Hamai & Hirayama (1979), and Nakayama & Watanabe (1964).

Table 3. Derived reaction rates for reactions R_3 and R_4 normalized to $r_h = 1$ AU by r_h^{-2}.

Date	R_3 [10^{-7} s^{-1}]	R_4 [10^{-7} s^{-1}]
23.11.1997	9.5 ± 2.4	195. ± 15.
6.12.1997	15.4 ± 5.1	202. ± 22.
19.12.1997	9.4 ± 0.5	200. ± 12.
20.1.1998	9.6 ± 3.2	202. ± 20.
21.1.1998	9.6 ± 6.1	199. ± 13.4
21.3.1998	9.4 ± 3.1	188. ± 20.0
17.8.1996	15.6 ± 4.1	143. ± 45.0
2.10.1996	8.9 ± 3.2	201. ± 15.0

From all isomeric forms of C_3H_4, C_3 is formed via the same intermediate product C_3H_2. As will be discussed later we are not able to quantify how much each of the isomeric forms contributes to the formation of C_3. We have therefore decided to use a general C_3H_4 molecule as the parent and have used medium reaction rates, which combine the reaction pathways for both isomers. This takes also into account the large uncertainty for each of the reaction rates. The additional error by using a medium reaction rate is considered in the error discussion later in this paper.

Jackson et al. (1992) discussed the implications of laboratory studies of the photochemistry of C_3H_2 on comet chemistry. Recently some laboratory work of the photodissociation cross sections of C_3H_2 has been published by Fahr et al. (1998). The data are still too sparse to determine a reaction rate for this process. For this reason, we used a different approach to obtain these reaction rates. The measurements of radial profiles of the C_3 radical at a number of heliocentric distances allow us to derive a good estimate for the two missing reaction rates.

The reaction rate for

$$R_3 : C_3H_2 \xrightarrow{h\nu} C_3 + H_2$$

is basically unknown and the reaction rate for the photodissociation of C_3

$$R_4 : C_3 \xrightarrow{h\nu} C_2 + C$$

is only based on estimates done, for example, by Huebner et al. (1992).

We have derived estimates by running the ComChem model with different combinations of possible reaction rates for the reactions R_3 and R_4. For each combination of reaction rates the best match between modeled and measured C_3 profile was derived. The global minimum in the χ^2 values marks the best fitting pair of reaction rates. It is determined using a bi-linear minimization routine (Press et al. 1992). The best fitting pair of reaction rates for reaction R_3 and R_4 is listed in Table 3 for each night.

The results for the photodissociation of C_3H_2 (R_3) agree within the errors over all observed nights. Two nights observed at the Danish 1.54 m telescope (6.12.1997 and 17.8.1996) show a deviation to higher values. This is most likely caused by the optical contamination of the C_3 profile. Therefore, to determine a mean value for the reaction rate, these two nights have been excluded. The derived mean is $R_3 = 9.5 \pm 0.3 \times 10^{-7}$ s^{-1}.

The results for the photodissociation of C_3 (R_4) agree also within the errors over all observed nights. Only the value obtained for the night 17.8.1996 shows a slight deviation, but for consistency with the calculations for R_3 the night 6.12.1997 was excluded as well. Since these data were obtained at the Danish 1.54 m telescope, the deviation is presumably caused by the contamination of the C_3 profile. Taking the mean value of the remaining nights, yields a reaction rate coefficient of $R_4 = 200.0 \pm 5.5 \times 10^{-7}$ s^{-1}.

For the electron impact dissociation of C_3H_4, there are no measurements available. In fact, even the reaction pathways are unclear. One might assume a similarity to the photodissociation reactions. Alman & Ruzic (2000) give some general estimates for branching ratios for electron impact dissociation. However, without measurements of electron impact reactions for any of the C_3H_4 isomers, it is nearly impossible to estimate reaction rates. As an estimate for the effect of electron impact dissociation on the formation of C_3, a hypothetical reaction

$$C_3H_4 + e \longrightarrow C_3 + H_2 + H_2 + e$$

was included in the reaction network. For this reaction, Schmidt et al. (1988) gives an estimate for an effective dissociation rate. This hypothetical reaction needs to be replaced by the individual electron impact dissociation reactions if reaction rates become available. In the error discussion (see below) the reaction rate has been varied by a factor of 10 to estimate the influence on the derived production rate of C_3, which has then been included in the error bar of the C_3 production rate.

Krasnopolsky (1991) proposed propynal (C_3H_2O) as another possible C_3 parent. The dissociation of propynal depends on the wavelength range considered. Krasnopolsky (1991) assumed that at 1216 Å the dissociation is similar to that of propyne with one oxygen atom (rather than two hydrogen atoms) removed in the first step. The asterisk marks an excited state.

$$C_3H_2O \xrightarrow{h\nu} C_3H_2^* + O$$
$$C_3H_2^* \longrightarrow C_3 + H_2$$

In the near ultraviolet region, the photodissociation occurs mainly via

$$C_3H_2O \xrightarrow{h\nu} CO + C_2H_2$$

The intensity of the solar flux is very low in this wavelengths range. Therefore, the total yield of C_3 produced from propynal is only approximately 0.01 compared to the production by C_3H_2 (Krasnopolsky 1991). For this reason, it has been neglected in this study.

5. The main chemical reaction network for the formation of C_2 and C_3

Based on a detailed analysis of the reaction network, it is possible to determine a main reaction network describing the formation of C_2 and C_3. The network is shown in Fig. 1. It is an important simplification compared to the over 200 reactions related to the hydrocarbon chemistry.

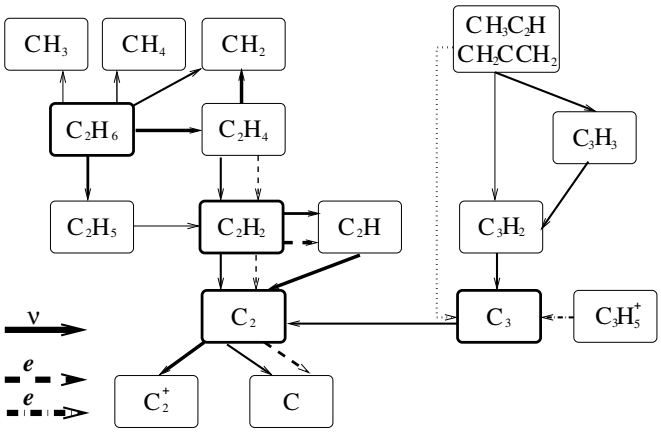

Fig. 1. Main reactions for the formation of the C_2 and C_3 radical. The thickness of the arrow indicates the importance of the reaction. The dotted arrow denotes the hypothetical reaction for the electron impact dissociation of C_3H_4. Thick boxes mark molecules that have been observed.

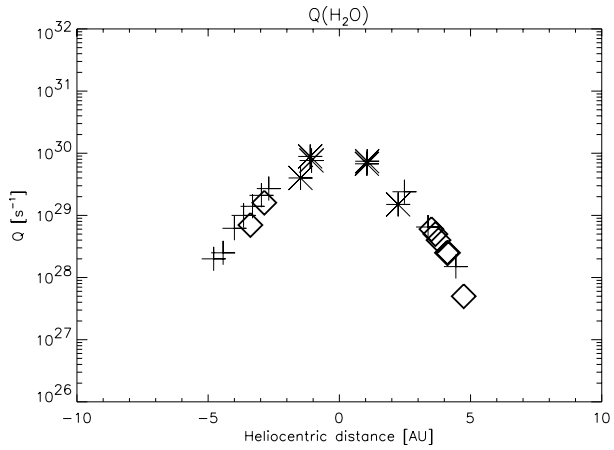

Fig. 2. Water production rate (diamonds) estimated for the model input and water production rates (crosses) measured by Weaver et al. (1999b) and (stars) Dello Russo et al. (2000).

The branch for the formation of C_2 consists of 18 reactions. The black arrows are photodissociation reactions, the gray arrows electron impact dissociation reactions.

Looking at the two parent molecules C_2H_2 and C_2H_6, it has been stated already that the main destruction pathway of C_2H_6 leads to C_2H_4 and CH_2. Therefore, C_2H_2 is the major source for the C_2 radical. This is in agreement with the fact that the abundance of C_2H_6 can be varied over a wider range than C_2H_2 without a significant effect on the modeled C_2 profile.

For the formation of the C_2 radical, photodissociation and electron impact dissociation of C_2H_2 play an approximately equally important role. This is a result of the high electron density which effectively forms C_2 by dissociation.

The main reaction network for the formation of C_3 contains, apart from photodissociation and electron impact dissociation, electron recombination of $C_3H_5^+$ also (light gray arrow). It should be reiterated, that the direct dissociation of C_3H_4 by electron impact is a hypothetical reaction. It seems more likely that the electron impact dissociation follows a similar pathway as the photodissociation.

The network has been simplified in the sense that allene and propyne are combined to a general C_3H_4 parent molecule. This simplification is made, since it is not possible to determine the abundance ratios of the two isomers from the measurements. The dissociation of allene and propyne both lead to the same intermediate product C_3H_2 from which C_3 is formed.

Finally a word of caution is necessary. The simplified reaction networks as given in Fig. 1 cannot replace the full chemistry network in general. The sole purpose of determining them is to find the main channels of formation and to support the error analysis. At other heliocentric distances, the relative importance of reactions may change significantly or reactions that are not even included in the simplified network might become important.

6. Model input: the nucleus – properties and composition

In order to run the ComChem model, the initial abundances within the coma have to be defined for each heliocentric distance used. The ComChem model as used in this study does not include a sublimation model. The modeling itself does not start on the nucleus surface, but in a shell above the Knudsen flow boundary layer (Huebner & Markiewicz 2000). In addition, as Huebner & Benkhoff (1999) pointed out, the abundances in the coma are not necessarily the same as in the nucleus. This is particularly true at large heliocentric distances, for species with a low volatility. Therefore instead of nucleus abundances the composition in the coma is given.

The composition used for this study consists of 22 species for comet Hale-Bopp as given in Bockelée-Morvan et al. (2000). For all species, the production rates have been interpolated, or if necessary extrapolated, to the heliocentric distance of the observation. For all species except water and CO_2, which have been observed within the distance range covered by our observations, the extrapolation assumed a $Q \sim r_h^b$ relationship with b constant over the whole range of heliocentric distances covered in this study.

There are only very few measurements for the water production rates available for heliocentric distances greater than 3 AU. From this distance outward, a severe decrease in the water sublimation is expected. Therefore the assumption of $Q(H_2O) \sim r_h^b$ with a constant b as used above is not valid for the extrapolation of water production rates to larger heliocentric distances. For this work a water sublimation model by Huebner & Benkhoff (1999) and Benkhoff & Huebner (1995) was used and scaled by a factor using the available measurements of $Q(H_2O)$. The model assumes a porous nucleus with water ice as the major component and a number of minor ice components with higher volatility. It assumes a Hale-Bopp-like orbit and orientation of the spin-axis. As can be seen in Fig. 2, this model is in good agreement with the values by Weaver et al. (1999b) and Dello Russo et al. (2000) for the post-perihelion measurements. Comet Hale-Bopp showed a slightly

higher water production pre-perihelion. However, the differences between the estimated and the measured production rates are less than a factor of 2. This has no significant effect on the results. The same model yields the surface temperature T_0 from the energy balance at the surface. However, this value has little influence on the modeling, since the temperature of the bulk gas is calculated within the model in a self-consistent way.

The production rates for CO_2 have been extrapolated based on the values obtained by Weaver et al. (1999b), assuming that the activity scales with heliocentric distance as CO.

For species which have not been observed at large heliocentric distances the production rates had to be estimated. It was assumed that the abundance ratio relative to Q(HCN) was constant for these species. As was shown in Rauer et al. (2003), HCN is the dominant parent of CN. Using this result, the production rate for the unknown species can then be estimated using Q(CN). The abundance ratios near perihelion were obtained from Bockelée-Morvan et al. (2000). Most of these species have a very low abundance and all of them play a negligible role in the chemistry for the formation of C_2 and C_3. Sensitivity tests have shown that even an error by an order of magnitude in the estimates of their production rates has no significant effect on the results. They are included for completeness as they might become important under different conditions, e.g., close to perihelion.

The ComChem model derives the velocity of the bulk gas in a self-consistent way. While the inner coma is collision dominated, molecules with a molecular weight close to the mean molecular weight of the bulk gas are thermalized quickly. At the nucleocentric distances considered in this work we can assume that all species considered are thermalized. The velocities of the bulk gas calculated with the ComChem model are in good agreement with the empirically determined evolution with heliocentric distance $v = 1.112 \cdot r_h^{-0.41}$ as given by Biver et al. (1997).

7. Deriving the production rates

The basic principle to derive abundances using the ComChem model is shown in Fig. 3. The ComChem model is used to generate model column density profiles for the C_2 and C_3 radicals and these are compared to the measured profiles. The nucleus composition is changed until modeled and measured profiles agree. In practice, this is done by two iterations, a first iteration for the C_3H_4 abundance and a second one for the C_2H_2 and C_2H_6 abundances. It is important to keep this order of iterations. Based on our extensive study of the chemistry, C_3H_4 is, via C_3, a grand-parent of C_2, while C_2H_2 and C_2H_6 have little or no influence on the C_3 formation.

The method is based on the assumption that C_3H_4 is the sole dominant parent molecule of the C_3 radical in this model, while C_2 has two main parent molecules and C_3 as a further minor parent. This has an important consequence. The abundance of C_3H_4 can be derived directly by adjusting the model abundance until the model yields a C_3 profile which is in agreement with the measurements. Tests show that the reaction rates mainly affect the shape of the profile, while the abundance of C_3H_4 yields a shift of the resulting profile. Therefore, it

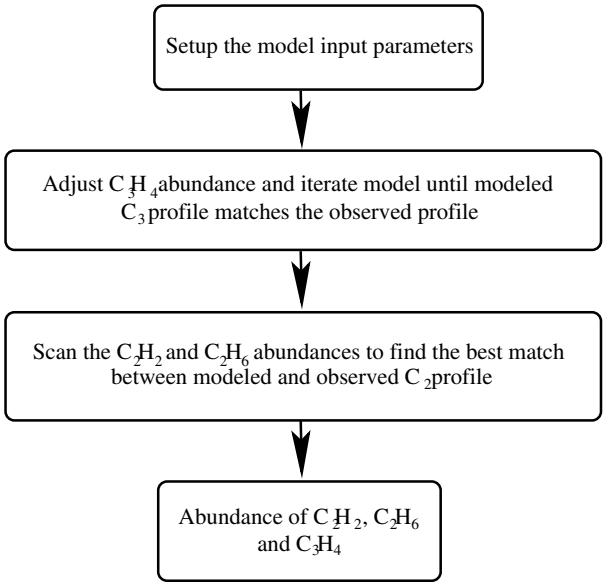

Fig. 3. Flowchart for obtaining abundance ratios using the ComChem model.

is possible to derive the reaction rates for the photodissociation of C_3H_2 and C_3 and the production rate for C_3H_4 in separate fits. The effects of variations of the reaction rates in the C_3 chemistry on the resulting C_3H_4 abundance are in the range of 30%. In a sense, the determination of C_3H_4 production rates used here is similar to using a multi-step Haser model.

For the C_2 parent molecules, however, the influence of the two main parent molecules has to be separated. Fortunately, the spatial column density profiles provide enough information for this task. The fit to the absolute values is mainly determined by the abundance, whereas the fit to the shape is governed by the abundance ratio of $Q(C_2H_2)$:$Q(C_2H_6)$. The abundance of both parent molecules is varied until the shape and the absolute column densities of the modeled profile fit the observed profile. Basically this is a two-dimensional parameter space which has to be scanned in a most effective way. The goodness of the fit is optimized by minimizing the scaling factor between modeled and measured profiles and by minimizing the χ^2 error as a measure for the fit to the shape of the profile.

Figures 4 and 5 show the best fitting profiles for each of the nights studied. In these plots triangles denote sunward, and diamonds tailward profiles. In this and all following plots and tables, negative heliocentric distances denote preperihelion observations. The radial profiles for C_3 are in general more noisy than the profiles for C_2. There is still a good agreement for C_3 over the whole range of heliocentric distances covered in this study. The C_2 modeled radial column density profiles show an excellent agreement with the observations over the whole range of heliocentric distances covered in this study.

8. Production rates for C_2H_2, C_2H_6 and C_3H_4

Combining all results from the model runs, the evolution of the abundances of the C_2 and C_3 parents with heliocentric distance can be studied. Production rates for C_2H_2, C_2H_6, and C_3H_4 have been determined in the heliocentric distance

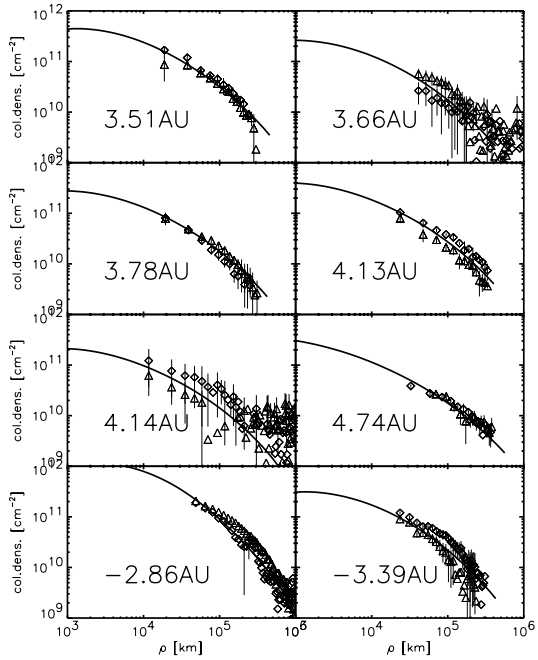

Fig. 4. Overview of the best fitting C_3 profiles (triangles – sunward, diamonds – tailward, negative heliocentric distances denote preperihelion observations).

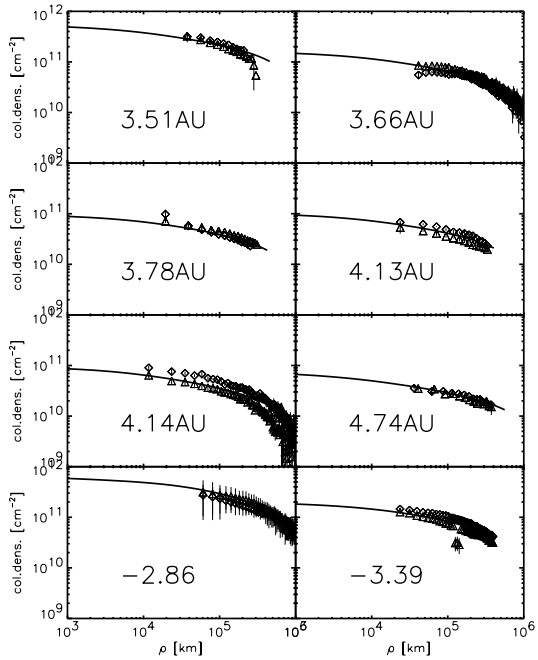

Fig. 5. Overview of the best fitting C_2 profiles (triangles – sunward, diamonds – tailward, negative heliocentric distances denote preperihelion observations).

range from 2.86−4.74 AU. Table 5 lists the production rates with the associated errors.

Figure 6 is a plot of the production rates of C_2H_2, C_2H_6, and C_3H_4 versus heliocentric distance. Pre- and postperi helion values derived in this work are plotted using different symbols (square for pre- and diamond for postperihelion) to show that there is no significant asymmetry around perihelion.

Table 5. Production rates for C_2H_2, C_2H_6 and C_3H_4 derived in this work - Negative heliocentric distances refer to preperihelion measurements.

Distance [AU]	C_2H_2 [10^{25} s^{-1}]	C_2H_6 [10^{25} s^{-1}]	C_3H_4 [10^{25} s^{-1}]
–3.39	120. ± 43.3	360. ± 178.	66.2 ± 40.1
–2.86	260. ± 91.6	520. ± 268.	20.2 ± 13.3
3.66	112. ± 39.1	340. ± 177.	54.6 ± 32.8
3.78	69.5 ± 24.2	100. ± 78.2	55.8 ± 33.7
4.1	82.5 ± 33.5	164. ± 127.	102. ± 70.2
4.14	77.3 ± 26.5	219.7 ± 117.	43.0 ± 26.5
4.74	64.3 ± 22.8	196.0 ± 108.	65.2 ± 41.1

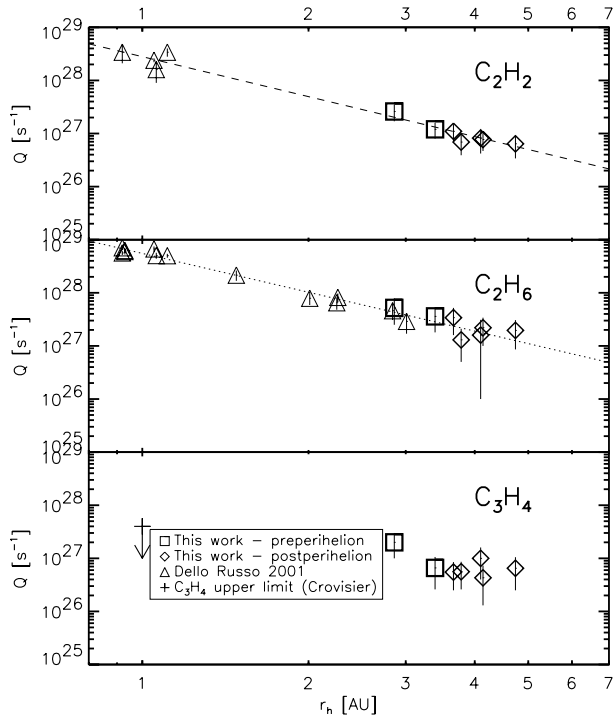

Fig. 6. Evolution of abundance ratios over heliocentric distance.

Also plotted are the C_2H_2 and C_2H_6 production rates (triangles) obtained by Dello Russo et al. (2001) from infrared observations. The dotted line is a fit to the production rates of C_2H_6 given by Dello Russo et al. (2001) and extrapolated to the distance range covered here. The values for the production rates of C_2H_6 determined in this work are in excellent agreement with this fit. For C_2H_2, the dashed line is a fit to the values for the production rates derived in this work. The extrapolation of this fit to small heliocentric distances is consistent with the values for C_2H_2 measured by Dello Russo et al. (2001) near perihelion.

The value of $Q(CH_3CCH) < 4 \times 10^{27}$ s^{-1} in Fig. 6 is a 3-σ upper limit derived for propyne by Crovisier (2000) from observations of the J 13-12 group of lines at 222.167 GHz. The observations have been obtained at the IRAM interferometer on March 18, 1997. The production rates for C_3H_4 obtained in this work are in agreement with this upper limit.

Unfortunately, none of the isomeric forms of C_3H_4 has been detected in a comet. Based on the study done here more complex parent molecules for C_3 as for example C_3H_6 or C_3H_8 can not be excluded. However these molecules would produce C_3 most likely via C_3H_4 as an intermediate step. If significant amounts of these molecules are present their dissociation rate has to be very fast in order to mimic a nucleus source of C_3H_4. While this is likely for the cyclic isomer as discussed above it seems unlikely for large C_3 containing molecules. We assume therefore that more complex parents form only a minor contribution within the errors derived for the production rate of C_3H_4.

9. Error discussion

With a comprehensive model like ComChem and an iterative approach as used in this study, it is difficult to derive physically meaningful errors. Therefore, we have used a sensitivity analysis based on a variation of the important parameters and quantify for each the influence on the production rates. We have identified the main sources of uncertainty as shown in Table 6. For each of these, we have performed a separate analysis. The table shows the range over which the parameters have been varied and an upper limit for the effect on the derived production rate.

To compute the final errors associated with the production rate for each of the observations, it is necessary to combine the estimates for the quantitative errors as listed in Table 6. As has been stated, these errors are upper limits for the effect of each uncertainty. The total error is a combination of each of these error terms. Because the errors are not independent the laws of error propagation are not valid here.

For $Q(C_2H_2)$ and $Q(C_2H_6)$, the combined error can be estimated to be ≈30%, while for $Q(C_3H_4)$ an error of ≈50% can be estimated. These estimates are based on a weighted average of the errors as listed in Table 6. The validity of these estimates has been tested by changing several parameters at the same time. The cumulative error was for all cases within the given estimates.

To derive absolute errors, the principle errors derived in this section are combined using the law of error propagation with the errors derived from the fitting procedure. The use of the law of error propagation is valid here because these two types of errors are strictly independent. The resulting errors are shown in Table 5 in Sect. 8.

10. Abundance ratios relative to water and carbon monoxide

Figure 7 shows the ratios of the production rates of C_2H_2, C_2H_6, and C_3H_4 relative to the water and CO production rates, plotted versus heliocentric distance. As neither H_2O nor CO production rates have been measured at the heliocentric distances of the C_2 and C_3 observations, the values used as input for the ComChem model have been adopted. For completeness, the values determined by Dello Russo et al. (2001) measured at perihelion have been included as well. This ratio to CO is in good agreement with the values derived in this work for larger heliocentric distances.

Table 6. Summary of the upper limits for the quantitative errors.

Variation of	varied by factor of	Upper limit for the error $Q(C_2H_2)$	$Q(C_2H_6)$	$Q(C_3H_4)$
Abundance of H_2O	2	10%	10%	5%
CO and CO_2 abundance	50%	20%	20%	10%
Abundance of minor species	10	5%	5%	5%
$C_2H_2+h\nu \rightarrow C_2+H_2$	5	10%	10%	
$C_2H_2+h\nu \rightarrow C_2H+H$	5	5%	5%	
$C_2H+h\nu \rightarrow C_2+H$	5	5%	5%	
$C_2H_2+e \rightarrow C_2+H_2$	10	10%	10%	
$C_2H_2+e \rightarrow C_2H+H$	10	20%	20%	
$C_3H_2+h\nu \rightarrow C_3+H_2$	5			30%
$C_3+h\nu \rightarrow C_2+C$	5			30%
$C_3H_4+e \rightarrow C_3+H_2$	10			50%
Remaining reaction rates	–	5%	5%	5%
Fit on profile	–	5%	5%	5%
Error on spatial profiles	–	10%	10%	10%

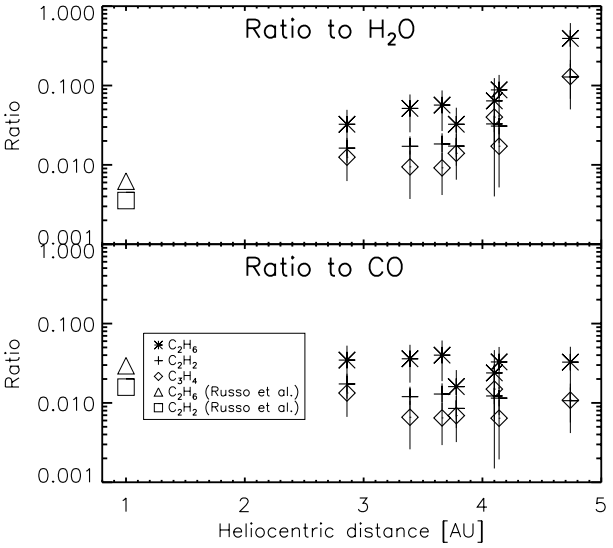

Fig. 7. Evolution of abundance ratios relative to water and to carbon monoxide over heliocentric distance.

Water is the main driver for cometary activity up to 3–4 AU heliocentric distance. At larger heliocentric distances, the main driver for cometary activity is carbon monoxide (CO). The upper panel of Fig. 7 shows a steep increase in the ratios of C_2H_2, C_2H_6, and C_3H_4 relative to H_2O for heliocentric distances greater than 3 AU where the water production rate decreases. The lower panel shows that the ratio relative to CO remains constant within the error bars up to 4.74 AU. The activity of C_2H_2, C_2H_6 and C_3H_4 at these distances is clearly

Table 7. Abundance ratios in comet Hale-Bopp relative to carbon monoxide derived in this work and upper limits for the abundance ratios relative to CO of solid acetylene and ethane in NGC 7538:IRS9 derived by Boudin et al. (1998).

Hale-Bopp (this work):		
$Q(C_2H_2)/Q(CO)$	=	0.01 ± 0.001
$Q(C_2H_6)/Q(CO)$	=	0.03 ± 0.004
$Q(C_3H_4)/Q(CO)$	=	0.008 ± 0.004
NGC 7538:IRS9 derived by Boudin et al. (1998):		
$Q(C_2H_2)/Q(CO)$	$\leq$	0.014
$Q(C_2H_6)/Q(CO)$	$\leq$	0.002

not controlled by water sublimation. For C_2H_2 and C_2H_6, this comes as no surprise because the sublimation temperatures for these pure ices are approximately 49 K and 52 K, respectively. Therefore, these molecules have a higher volatility than water. The ratio of the C_3H_4 production rate to the water production rate suggests that C_3H_4 is also a highly volatile species. Up to now, there are very few data on the volatility of allene or propyne. However, the existing measurements indicate also a high volatility, supporting the identification of these molecules as possible C_3 parents.

Table 7 shows the derived ratios and the associated errors in comparison with the upper limits for the ratios of C_2H_2 and C_2H_6 relative to CO in NGC 7538:IRS9 as determined by Boudin et al. (1998). According to Werner et al. (1979), this is a massive protostellar object with an associated infrared reflection nebula deeply embedded in a dense molecular cloud. It has been well studied in the entire mid-infrared range from ground based observatories and by the Infrared Space Observatory (e.g. Allamandola et al. 1992; Whittet et al. 1996). While the ratio for C_2H_2 to CO is in agreement with the value derived for comet Hale-Bopp, the upper limit for C_2H_6 to CO indicates an enrichment of ethane in comet Hale-Bopp. However one has to be careful by comparing with only one protostellar region. Unfortunately, only very few measurements of the abundance of hydrocarbons in dense molecular clouds are available.

11. Abundance ratios relative to acetylene

Figure 8 shows the evolution of the abundance ratio of ethane relative to acetylene over heliocentric distance. The ratio is constant, within the errors, over the whole range of heliocentric distances covered in this study. From the measurements in this work, a mean ratio of $Q(C_2H_6)/Q(C_2H_2) = 2.3 \pm 1.0$ can be derived. This value shows clearly that comet Hale-Bopp is overabundant in ethane compared to acetylene. The derived ratio is in agreement with the value of $Q(C_2H_6)/Q(C_2H_2) = 2.4 \pm 0.7$ derived by Dello Russo et al. (2001) for comet Hale-Bopp at perihelion.

Table 8 shows the abundance ratio determined in this work in comparison to ratios derived for other comets. Three other long-period comets also show a similar high abundance of ethane. Only comet C/1999 S4 might be depleted in ethane relative to acetylene, but in this case only a lower limit has been

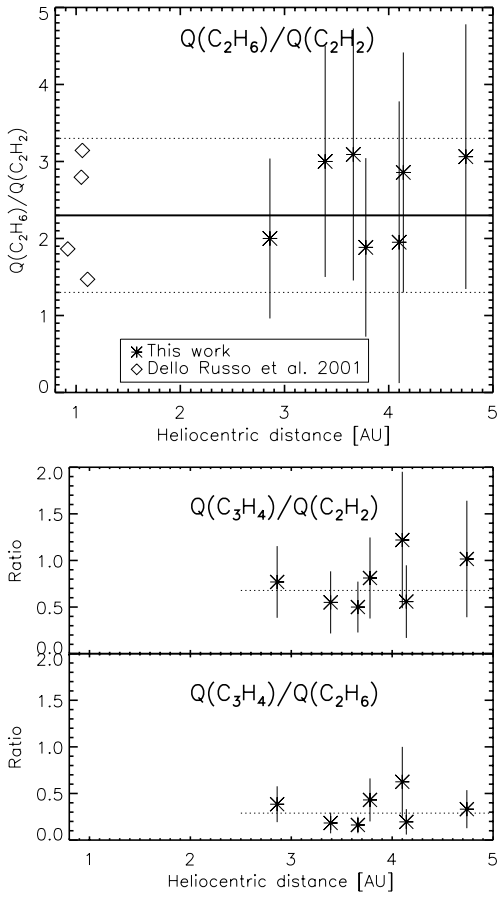

Fig. 8. *Upper panel*: abundance ratio of C_2H_6 relative to C_2H_2 versus heliocentric distance. The solid line is the mean value derived in this work, the dotted lines show the associated error. The values determined by Dello Russo et al. (2001) are displayed for comparison. *Lower panel*: evolution of the abundance ratios of C_3H_4 to C_2H_2 and C_2H_6 vs. heliocentric distance, the dotted lines are the derived mean values.

derived. However, this comet seems to be depleted in many other volatile species as well (Mumma et al. 2001).

Mumma et al. (2000) reported the detection of ethane in comet Giacobini-Zinner, a probable Kuiper-belt comet. Their measurements indicate that this comet was depleted in C_2H_6. Weaver et al. (1999a) did not detect C_2H_6 in this comet and derived an upper limit for the production rate of C_2H_6 which was lower than the production rate derived by Mumma.

The ratios obtained in this work and the values determined for other Oort cloud comets indicate that an overabundance of ethane is the rule and not the exception for this class of comets. The statistical base is still too small to draw any similar conclusions on the chemical composition of Kuiper-belt comets.

The possible implications for the formation of the nucleus of comet Hale-Bopp will be discussed later.

Based on the production rates derived for C_3H_4 in this work, it is possible for the first time to estimate abundance ratios for C_3H_4 relative to C_2H_2 and C_2H_6. The ratios are constant within the errors over the whole heliocentric distance range studied in this work. C_3H_4 seems to be less abundant than the other two species. Unfortunately, none of the isomeric

Table 8. Abundance ratio of ethane relative to acetylene derived in this work and for some comets (Dello Russo et al. 2001).

Comet	$Q(C_2H_6)/Q(C_2H_2)$
Hale-Bopp (this work)	**2.3 ± 1.0**
Hale-Bopp	2.4 ± 0.7
C/1996 B2	~0.5−4
Hyakutake	4 ± 2
Lee	2.6 ± 0.3
C/1999 S4 Linear	>0.9

Table 9. Abundance ratios of C_3H_4 to C_2H_2 and C_2H_6.

$Q(C_3H_4)/Q(C_2H_2)$	=	0.65 ± 0.37
$Q(C_3H_4)/Q(C_2H_6)$	=	0.28 ± 0.18

forms of C_3H_4 has been identified in a comet coma. The fact that C_3H_4 is less abundant than C_2H_2 and C_2H_6 might be due to an observational problem. The observational problems have been discussed by Dello Russo et al. (2001). The energy is distributed over many lines in the radio range, therefore the strength of an individual line is low. At infrared wavelengths, there is a blend between the C_3H_4 emission lines and the broad emissions of the CH-bending modes. Still, the abundance ratio of C_3H_4 might set limits to the formation region of comet Hale-Bopp as will be discussed below.

12. Clues on the formation region of comet Hale-Bopp

The abundance ratios for the C_2 and C_3 parent molecules derived in this study can give clues to the formation region of comet Hale-Bopp. To be more precise, it can give clues on the formation region of the ice mixture forming the nucleus. Within the heliocentric distance range covered in this study no obvious inhomogeneities in the C_2 or C_3 production rate have been observed. Therefore it seems valid to assume that the nucleus of comet Hale-Bopp is chemically homogeneous at least for the shell sublimated during this perihelion passage.

In order to study the formation region, we have compared the derived values for comet Hale-Bopp with measurements in the interstellar medium wherever possible. We also took a closer look on possible scenarios for the formation of C_2H_2, C_2H_6, and C_3H_4 in the early stage of the solar system.

A direct comparison is difficult because C_2H_2 and C_2H_6 ice have not yet been detected in the interstellar medium. The problem in observing solid C_2H_2 and C_2H_6 ices is a blend with the signature of H_2O ice which masks the C_2H_6 and C_2H_2 bands (Boudin et al. 1998). Only upper limits for their abundances can be derived. Of course, the ratio of the upper limits for $Q(C_2H_2)$ and $Q(C_2H_6)$ is not directly comparable with the abundance ratio of $Q(C_2H_2)$ to $Q(C_2H_6)$ as derived in this study, although this has been done in the literature. A better approach is to compare the abundance ratios of C_2H_2 and C_2H_6 relative to CO with the upper limits derived for the interstellar medium.

In this paper, an abundance ratio of C_2H_2 relative to CO of $Q(C_2H_2)/Q(CO) = 0.01 \pm 0.004$ was determined. This is in agreement with the upper limit for the dense molecular cloud NGC 7538:IRS9 as determined by Boudin et al. (1998).

In molecular clouds, C_2H_2 is formed by gas-phase ion-molecule reactions. Lahuis & van Dishoeck (2000) have reported the observation of C_2H_2 in the gas phase toward a number of massive young stellar objects. Strong evidence for the presence of C_2H_2 ice on grain surfaces is the enhanced abundance of C_2H_2 in the gas phase toward the warmer regions of dense molecular clouds (Lahuis & van Dishoeck 2000). This C_2H_2 is most probably formed by sublimation of ice from grain surfaces. Lahuis and van Dishoeck derived under this assumption an abundance ratio of C_2H_2 to water ice of $\sim(1-5) \times 10^{-3}$. This is in rough agreement with the values of $(6.23 \pm 0.42) \times 10^{-3}$ obtained for Hale-Bopp at perihelion by Dello Russo et al. (2001).

For the abundance ratio of C_2H_6 relative to CO, a value of $Q(C_2H_2)/Q(CO) = 0.03 \pm 0.01$ was determined in this work. This is about an order of magnitude larger than the value of $Q(C_2H_6)/Q(CO) \leq 0.002$ as determined by Boudin et al. (1998) for NGC 7538:IRS9 (see above). This indicates that C_2H_6 is indeed overabundant in comet Hale-Bopp compared to a dense molecular cloud which is similar to the precursor of our solar system (Boudin et al. 1998). One possible explanation for this enrichment is formation of C_2H_6 during the early stage of our solar system.

For such formation there are at least two possible scenarios. At low temperature, $T = 10-50$ K, C_2H_6 cannot be formed by gas-phase chemistry because all relevant reactions are endothermic (Herbst 1983). However, in this temperature range grain surface chemistry is very efficient. Moore & Hudson (1998) and Cottin et al. (1999) showed that ices consisting of mixtures of H_2O+C_2H_2 and H_2O+CH_4+C_2H_2 can produce C_2H_6 efficiently when irradiated with UV or gamma rays. According to Hiraoka et al. (2000) the yield of C_2H_6 is largely enhanced at temperatures below $T < 35$ K and the process is most efficient at temperatures of about 10 K (Box 1 and 2 in Fig. 9). Moore and Hudson noted also that no C_2H_2 was formed in a significant amount in any of their experiments. This would be consistent with a pristine origin of C_2H_2. Furthermore, only trace amounts of C_2H_4 are detected in these experiments. While C_2H_4 is formed by hydrogenation of C_2H_2 it is even more efficient in adsorbing additional H atoms than C_2H_2. Therefore C_2H_4 is only an intermediate step in the formation of C_2H_6 from C_2H_2. This is consistent with the fact that no C_2H_4 has been detected in comets. As discussed by Mumma et al. (1996), the formation of C_2H_6 by hydrogenation of C_2H_2 on grain surfaces could indeed be a possible explanation for the high abundance of C_2H_6 relative to C_2H_2 as observed in comet Hale-Bopp.

While C_2H_6 cannot be formed by gas-phase chemistry at low temperature, Notesco et al. (1997) noted that it can be formed by CH_4 photolysis under high temperature ($T \gtrsim 100$ K) and high density conditions (Box 3 in Fig. 9). These conditions can be found in the Jupiter region of the protoplanetary disk.

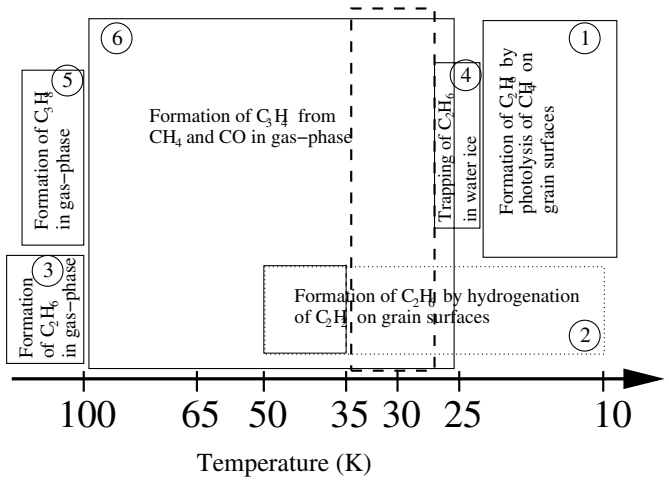

Fig. 9. Temperature ranges for the formation processes of C_2H_2, C_2H_6 and C_3H_4. The numbers in the boxes are referenced in the text. 1 and 2 denote areas with formation on grain surfaces (the solid part in box 2 is less effective than the dotted part), 3, 5, and 6 denote formation in the gas-phase. 4 shows an enrichment by trapping in amorphous water ice. The dashed box shows the likely range of formation temperatures.

The overabundance of C_2H_6 can also be explained by a very efficient trapping of C_2H_6 in amorphous water ice. While Notesco et al. (1997) originally assumed this process would be most efficient at 64−66 K, new work by the same group (Notesco et al. 2003) indicate a temperature around 25 K (Box 4 in Fig. 9). However, even though amorphous water ice may be present, it has not been detected in comets or in the interstellar medium. An open question in this scenario is the achievable C_2H_6 to CH_4 ratio. While Bar-Nun (1979) found a ratio $>1.5\times10^{-2}$, Mumma et al. (1996) (and references therein) state that the C_2H_6 to CH_4 ratio is $<10^{-3}$. Assuming this low ratio, the trapping of C_2H_6 in water ice would not be efficient enough to explain the overabundance of C_2H_6. Further laboratory and theoretical work is urgently needed on this topic.

Notesco et al. (1997) predict also the formation of C_3H_8 with an abundance comparable to C_2H_6 (Box 5 in Fig. 9).

Based only on the abundance of C_2H_6 relative to C_2H_2, it is difficult to decide between the two formation scenarios for C_2H_6 and therefore between two possible formation regions for the nucleus of comet Hale-Bopp. In this work, however, the abundance ratios of C_3H_4 relative to C_2H_2 and C_2H_6 could be estimated for the first time in a comet coma. Aikawa et al. (1999) showed in their numerical simulations of the evolution of molecular abundances in protoplanetary disks that C_3H_4 is readily formed by gas-phase chemistry from CH_4 and CO (Box 6 in Fig. 9). The relative yield is largely increased in the inner regions of the disks for $r_h \leq 20$ AU. In this region, the temperatures are high enough to sublime large amounts of CH_4 and CO from the icy mantles of dust grains. Outside the sublimation front of CH_4 and CO, the C_3H_4 abundance decreases rapidly with heliocentric distance.

With this additional information, the formation of C_2H_6 by hydrogenation on grain surfaces seems more likely. In this paper, values of $Q(C_3H_4)/Q(C_2H_2) = 0.65 \pm 0.37$ and $Q(C_3H_4)/Q(C_2H_6) = 0.28 \pm 0.18$ have been estimated. This indicates that C_3H_4 is slightly underabundant compared to C_2H_2 and C_2H_6. However, as discussed before, the formation of C_3H_4 is more efficient for higher temperatures (Aikawa et al. 1999). If the nucleus of Hale-Bopp was formed at temperatures ≥65 K, one would expect a high abundance of C_3H_4. Furthermore, formation of C_3H_8 would be expected in this scenario. There has been no detection of C_3H_8 in comet Hale-Bopp or any other comet yet. It has been searched for by Dello Russo et al. (2001) but they were unable to obtain an upper limit because of difficulties in observing the possible C_3H_8 emission bands.

On the other hand, the formation of C_2H_6 on grain surfaces for temperatures below 50 K, would be in agreement with the slight underabundance of C_3H_4. In the temperature range between 25 K and 50 K the formation of C_3H_4 is possible but not very efficient while the formation of C_2H_6 is possible and efficient. A lower limit for the temperature is in the case given by the sublimation temperature of CO at 24 K. Considering that C_2H_6 is clearly overabundant in comet Hale-Bopp one might even consider an upper limit for the formation temperature at $T \approx 35$ K, because the efficiency for the formation on grain surfaces is largely increased below this temperature as Hiraoka et al. (2000) have shown.

Therefore, based on the abundance ratios of C_2H_2, C_2H_6 and C_3H_4 derived in this work, a temperature range of $T \approx 25-35$ K seems likely for the formation of the nucleus of comet Hale-Bopp. This range has been marked by a dashed box in Fig. 9. This temperature range is in agreement with the results by several other groups giving a formation temperature for comet Hale-Bopp of $T \sim 30$ K. These results are based on different observational methods. For example, Crovisier (1997) based his results on the H_2O ortho-para ratio, Krasnopolsky et al. (1997) based theirs on the abundances of the noble gas Neon Meier et al. (1998) based theirs on the D/H ratio and recently Stern et al. (2000) based theris on the detection of Argon in the coma of comet Hale-Bopp.

Based on the results of this work and in combination with previous studies, there are some indications for the assumption that comet Hale-Bopp has been formed in a range from 10−30 AU from the early Sun. This would put the birthplace of comet Hale-Bopp somewhere in the region between Saturn and Uranus. However, the whole argumentation is based on a number of assumptions and poorly known quantities. While a high degree of uncertainty remains, the discussion presented here shows how the observations of radicals could be used to deduce informations about the nucleus and its formation.

13. Summary

The aim of this study is to analyze the formation of C_2 and C_3 in a comet coma at large heliocentric distances. For this purpose a chemical model for the formation of C_2 and C_3 from C_2H_2, C_2H_6, and C_3H_4 is presented based on the observations of C_2 and C_3 column densities obtained during the optical longterm-monitoring program of comet Hale-Bopp (Rauer et al. 2003). The chemical model was developed using and extending the

ComChem model by Huebner and Boice (Giguere & Huebner 1978; Boice et al. 1986, 1998; Huebner et al. 1987; Schmidt et al. 1988).

The chemical model contains an up-to-date reaction network to study the formation processes of the C_2 and C_3 radicals in a comet coma. At the heliocentric distance range $r_h >$ 2.86 AU covered in this study, the formation of the C_2 radical is dominated by photodissociation and electron impact dissociation of C_2H_2. C_2H_6 has been identified as a minor parent of C_2.

The observed C_3 column density profiles can be explained by C_3H_4 as the parent molecule. However, it is not possible to distinguish between the isomeric forms, allene and propyne. Both isomers can form C_3 via the same intermediate product C_3H_2. C_3 is formed by electron impact and photodissociation reactions. Although the reaction network for the formation of C_3 shows good agreement with the observed C_3 column density profiles it is still preliminary. It is based on reaction rates for the photodissociation of C_3H_2 and C_3, which had to be derived in this work from fits to the observed data. The reaction pathways for the electron impact dissociation of allene and propyne are still unknown. For this reason, a hypothetical reaction is included describing the direct dissociation of C_3H_4 by electron impact to form C_3. Due to all these uncertainties, the results for C_3 and its parent C_3H_4 have not the same quality as the results for C_2 and its parents C_2H_2 and C_2H_6. Nevertheless, the C_3 formation model presented here is the first model to include a detailed photochemical reaction scheme, in addition to a simplified electron impact reaction, linking allene and propyne with C_3.

The chemical model allows us to derive the abundances for C_2H_2, C_2H_6 and C_3H_4 using the observations of the C_2 and C_3 radicals in the optical wavelength range. The derived production rates for C_2H_2 and C_2H_6 are in very good agreement with values obtained by Dello Russo et al. (2001) from infrared observations at heliocentric distance $r_h \leq 3$ AU. The derived C_3H_4 production rate is consistent with an upper limit for propyne derived by Crovisier (2000) near perihelion. The values presented here extend the heliocentric distance range over which hydrocarbons can be studied in the coma of comet Hale-Bopp to almost 5 AU, a range presently not accessible by direct infrared observations.

The abundance ratios of C_2H_2, C_2H_6, and C_3H_4 relative to water and carbon monoxide have been studied for large heliocentric distances. They show that the abundance of C_2H_2 relative to carbon monoxide is comparable to interstellar molecular clouds, while the C_2H_6 to CO ratio indicates an overabundance in comet Hale-Bopp. Furthermore, the abundance ratios show that all three molecules have a high volatility. This is especially noteworthy for C_3H_4. Little is known about the volatility of allene or propyne, but the values for the latent heat of this molecules indicate a high volatility. This would be in agreement with the almost constant ratio of C_3H_4 to CO derived in this study.

It was possible for the first time to derive abundance ratios of C_3H_4 relative to C_2H_2 and C_2H_6. The values have a large uncertainty, because they include all uncertainties in the modeling of the C_2 and C_3 formation. Nevertheless, they are an important indicator showing that C_3H_4 is underabundant by a factor of about 2 compared to C_2H_2 and C_2H_6.

Using the results from the modeling, an attempt was made to derive indications for the formation region of comet Hale-Bopp. The idea was primarily to show how abundance ratios for C_2H_2, C_2H_6, and C_3H_4 determined with the model for the formation of C_2 and C_3 allows us to derive conclusions about the conditions during the formation of the nucleus of comet Hale-Bopp. A distance range of approximately 10−30 AU from the early Sun has been proposed as a possible formation region. However, one has to be very careful with this estimate, as it is based on a number of assumptions.

Finally it has to be pointed out, that the results for the formation chemistry of C_2 and C_3 are strictly valid only for comet Hale-Bopp and only in the heliocentric distance range covered in this study. Closer to the Sun other reactions may become increasingly important, due to the increase in solar insolation and due to the higher densities in the coma. Although the agreement with measurements by Dello Russo et al. (2001) implies that this has little effect on production rates of C_2H_2 and C_2H_6. Of special interest are short period comets and carbon-chain depleted comets, as these might have formed in a different region of the early solar system. Based on the classification by A'Hearn et al. (1995) Hale-Bopp was a normal comet. Other comets like comet 67P/Churyumov-Gerasimenko, the target of the Rosetta mission, appear to be depleted in C_2 and C_3 (Osip et al. 1992; Weiler et al. 2004). It would be especially interesting if both of the discussed C_2 parent molecules in these comets are depleted. If we assume that most of the C_2H_2 in a comet nucleus is of pristine origin, it seems more likely that carbon-chain depleted comets are only depleted in C_2H_6. This would indicate a different formation region in which the conversion of C_2H_2 to C_2H_6 was less effective or was stopped at an earlier time. The same is true for C_3 if we assume that C_3H_4 is the main parent. This molecule is most likely not of pristine origin and a depletion would give an indication on the formation conditions.

Acknowledgements. The author has been support by the German Research Council (DFG) under Grant HR714/2-3. This material is based upon work supported by the National Science Foundation under Grant No. 9973186.

References

A'Hearn, M. F., Millis, R. L., Schleicher, D. G., Osip, D. J., & Birch, P. V. 1995, Icarus, 118, 223

Aikawa, Y., Umebayashi, T., Nakano, T., & Miyama, S. M. 1999, ApJ, 519, 705

Allamandola, L. J., Sandford, S. A., Tielens, A. G. G. M., & Herbst, T. M. 1992, ApJ, 399, 134

Alman, D. A., & Ruzic, D. N. 2000, Phys. Plasmas, 7, 1421

Bar-Nun, A. 1979, Icarus, 38, 180

Benkhoff, J., & Huebner, W. F. 1995, Icarus, 114, 348

Biver, N., Bockelée-Morvan, D., Colom, P., et al. 1997, Earth Moon and Planets, 78, 5

Bockelée-Morvan, D., Lis, D. C., Wink, J. E., et al. 2000, A&A, 353, 1101

Boice, D. C. 2000, personal communication

Boice, D. C., Huebner, W. F., Keady, J. J., Schmidt, H. U., & Wegmann, R. 1986, Geophys. Res. Lett., 13, 381
Boice, D. C., Huebner, W. F., Keady, J. J., Schmidt, H. U., & Wegmann, R. 1998, in Comet Encounters, 206
Boudin, N., Schutte, W. A., & Greenberg, J. M. 1998, A&A, 331, 749
Brooke, T. Y., Tokunaga, A. T., Weaver, H. A., et al. 1996, Nature, 383, 606
Calvert, J. G., & Pitts, J. N. 1966, Photochemistry (New York: John Wiley & Sons)
Cochran, A. L. 1985, AJ, 90, 2609
Cottin, H., Gazeau, M. C., & Raulin, F. 1999, Planet. Space Sci., 47, 1141
Crovisier, J. 1997, Earth Moon and Planets, 79, 125
Crovisier, J. 2000, personal communication
Dello Russo, N., Mumma, M. J., DiSanti, M. A., et al. 2000, Icarus, 143, 324
Dello Russo, N., Mumma, M. J., DiSanti, M. A., Magee-Sauer, K., & Novak, R. 2001, Icarus, 153, 162
Donati, G. B. 1864, Astron. Nachr., 62, 378
Douglas, A. E. 1951, ApJ, 114, 466
Faber, D., Heinecke, U., Müller, T., et al. 2001, Eur. J. Org. Chem., 663
Fahr, A., Hassanzadeh, P., & Atkinson, D. B. 1998, J. Chem. Phys., 236, 43
Fahr, A., & Nayak, A. 1996, J. Chem. Phys., 203, 351
Fuke, K., & Schnepp, O. 1979, Chem. Phys, 38, 211
Giguere, P. T., & Huebner, W. F. 1978, ApJ, 223, 638
Halpern, J. B., Miller, G. E., & Okabe, H. 1988, J. Photochem. Photobiol. A: Chem., 42, 63
Hamai, S., & Hirayama, F. 1979, J. Chem. Phys., 71, 2934
Helbert, J. 2003, Ph.D. Thesis, Free University of Berlin
Herbst, E. 1983, ApJS, 53, 41
Hiraoka, K., Takayama, T., Euchi, A., Handa, H., & Sato, T. 2000, ApJ, 532, 1029
Huebner, W. F., & Benkhoff, J. 1999, Space Sci. Rev., 90, 117
Huebner, W. F., Keady, J. J., Boice, D. C., Schmidt, H. U., & Wegmann, R. 1987, Chemico-Physical models of cometary atmospheres, ed. M. S. Vardya, & S. P. Tarafdar, IAU Coll., 120, 431
Huebner, W. F., Keady, J. J., & Lyon, S. P. 1992, Ap&SS, 195, 1, see also: http://amop.space.swri.edu
Huebner, W. F., & Markiewicz, W. J. 2000, Icarus, 148, 594
Huggins, W. 1867, MNRAS, 27, 288
Jackson, W. M. 1976, J. Photochem., 5, 107
Jackson, W. M., Anex, D. S., Continetti, R. E., Balko, B., & Lee, Y. T. 1991, J. Chem. Phys, 95, 7327
Jackson, W. M., Bao, Y., Urdahl, R. S., et al. 1992, in ACM Proceedings
Jackson, W. M., Blunt, V., Lin, H., et al. 1996, Ap&SS, 236, 29
Job, V. A., & King, G. W. 1966, J. Molecular Spectroscopy, 19, 155
Krasnopolsky, V., Mumma, M. J., Abbott, M., et al. 1997, Science, 277, 1488
Krasnopolsky, V. A. 1991, A&A, 245, 310
Lahuis, F., & van Dishoeck, E. F. 2000, A&A, 355, 699
Lias, S. G., Collin, G. J., Rebbert, R. E., & Ausloos, P. 1970, J. Chem. Phys., 52, 1841
Mebel, A. M., Jackson, W. M., Chang, A. H. H., & Lin, S. H. 1998, J. Amer. Chem. Soc., 120, 5751
Meier, R., Owen, T. C., Jewitt, D. C., et al. 1998, Science, 279, 1707
Moore, M. H., & Hudson, R. L. 1998, Icarus, 135, 518
Moses, J. 2000, personal communication
Mumma, M. J., DiSanti, M. A., Dello Russo, N., et al. 1996, Science, 272, 1310
Mumma, M. J., DiSanti, M. A., Dello Russo, N., Magee-Sauer, K., & Rettig, T. W. 2000, ApJ, 531, L155
Mumma, M. J., Dello Russo, N., DiSanti, M. A., et al. 2001, Science, 292, 1334
Nakayama, T., & Watanabe, K. 1964, J. Chem. Phys., 40, 558
Notesco, G., Laufer, D., & Bar-Nun, A. 1997, Icarus, 125, 471
Notesco, G., Bar-Nun, A., & Owen, T. 2003, Icarus, 162, 183
Osip, D. J., Schleicher, D. G., & Millis, R. L. 1992, Icarus, 98, 115
Pang, K. D., Ajello, M. J., & Franklin, B. 1987, J. Chem. Phys., 86, 2750
Pouilly, B., Robbe, J. M., Schamps, J., & Roueff, E. 1983, J. Phys. B: Atom. Mol. Phys., 16, 437
Press, W. H., Teukolsky, S. A., Vetterling, W., & Flannery, B. P. 1992, Numerical Recipes in C, The Art of Scientific Computing, 2nd ed. (Cambridge University Press)
Rabalais, J. W., McDonald, J. M., Scherr, V., & McGlynn, S. P. 1971, Chem. Rev., 71, 73
Rauer, H., Arpigny, C., Boehnhardt, H., et al. 1997, Science, 275
Rauer, H., Helbert, J., Arpigny, C., et al. 2003, A&A, 397, 1109
Schmidt, H. U., Wegmann, R., Huebner, W. F., & Boice, D. C. 1988, Comput. Phys. Commun., 49, 17
Seki, K. 1985, Ph.D. Thesis, University of Tokyo
Stern, S. A., Slater, D. C., Festou, M. C., et al. 2000, ApJ, 544, L169
Stief, J. L., DeCarlo, V. J., & Payne, W. A. 1971, J. Chem. Phys., 54, 1913
Stief, L. J., Donn, B., Glicker, S., Gentieu, E. P., & Mentall, J. E. 1972, ApJ, 171, 21
Sutcliffe, L. H., & Walsh, A. D. 1952, J. Can. Chem. Soc.
Swings, P. 1965, QJRAS, 6, 28
Tokunaga, A. T., Brooke, T. Y., Weaver, H. A., Crovisier, J., & Bockelee-Morvan, D. 1996, IAU Circ., 6378, 1
Weaver, H. A., Chin, G., Bockelée-Morvan, D., et al. 1999a, Icarus, 142, 482
Weaver, H. A., Feldman, P. D., A'Hearn, M. F., et al. 1999b, Icarus, 141, 1
Weiler, M., Rauer, H., & Helbert, J. 2004, A&A, 414, 749
Werner, M. W., Becklin, E. E., Gatley, I., et al. 1979, MNRAS, 188, 463
Whittet, D. C. B., Schutte, W. A., Tielens, A. G. G. M., et al. 1996, A&A, 315, L357
Wodtke, A. M., & Lee, Y. T. 1985, J. Chem. Phys., 89, 4744
Wu, C. Y. R. 2000, personal communication
Yamamoto, T. 1981, Moon, Planets, 24, 453

Online Material

Table 4. The main reactions and their reaction rates. The † marks reactions for which rate coefficients have been derived in this work. Coefficients which have been derived during this work are printed in bold, while previous estimates for these coefficients are printed in italics.

Reactants				Products					Rate coefficent [s^{-1}]	Reference
C_2H_6	+	$h\nu$	$\longrightarrow$	C_2H_5	+	H			3.28×10^{-6}	(Huebner et al. 1992)
C_2H_6	+	$h\nu$	$\longrightarrow$	C_2H_4	+	H_2			3.67×10^{-6}	(Huebner et al. 1992)
C_2H_6	+	$h\nu$	$\longrightarrow$	CH_3	+	CH_3			8.80×10^{-7}	(Huebner et al. 1992)
C_2H_6	+	$h\nu$	$\longrightarrow$	CH_2	+	CH_4			2.22×10^{-6}	(Huebner et al. 1992)
C_2H_5	+	$h\nu$	$\longrightarrow$	C_2H_2	+	H_2	+	H	1.00×10^{-6}	(Boice 2000, pers. comm.)
C_2H_4	+	$h\nu$	$\longrightarrow$	C_2H_2	+	H_2			2.40×10^{-5}	(Huebner et al. 1992)
C_2H_4	+	$h\nu$	$\longrightarrow$	C_2H_2	+	H	+	H	2.30×10^{-5}	(Huebner et al. 1992)
C_2H_4	+	$h\nu$	$\longrightarrow$	CH_2	+	CH_2			6.00×10^{-5}	(Huebner et al. 1992)
C_2H_2	+	$h\nu$	$\longrightarrow$	C_2	+	H_2			2.74×10^{-6}	(Huebner et al. 1992)
C_2H_2	+	e	$\longrightarrow$	C_2	+	H_2	+	e	1.90×10^{-8}	(Schmidt et al. 1988)
C_2H_2	+	$h\nu$	$\longrightarrow$	C_2H	+	H			1.02×10^{-5}	(Huebner et al. 1992)
C_2H_2	+	e	$\longrightarrow$	C_2H	+	H	+	e	1.90×10^{-8}	(Schmidt et al. 1988)
C_2H	+	$h\nu$	$\longrightarrow$	C_2	+	H			3.00×10^{-5}	(Huebner et al. 1992)
C_2	+	$h\nu$	$\longrightarrow$	C	+	C			1.40×10^{-7}	(Huebner et al. 1992)
C_2	+	$h\nu$	$\longrightarrow$	C_2^+	+	e			9.10×10^{-7}	(Huebner et al. 1992)
C_2	+	e	$\longrightarrow$	C	+	C	+	e	9.43×10^{-10}	(Schmidt et al. 1988)
C_3H_4	+	$h\nu$	$\longrightarrow$	C_3H_3	+	H			1.33×10^{-4}	Moses (2000, pers. comm.)
C_3H_4	+	$h\nu$	$\longrightarrow$	C_3H_2	+	H_2			2.96×10^{-5}	Moses (2000, pers. comm.)
C_3H_4	+	e	$\longrightarrow$	C_3	+	H_2	+	H_2 + e	3.80×10^{-8}	(Schmidt et al. 1988)
C_3H_3	+	$h\nu$	$\longrightarrow$	C_3H_2	+	H			1.82×10^{-3}	Moses (2000, pers. comm.)
† C_3H_2	+	$h\nu$	$\longrightarrow$	C_3	+	H_2			$\mathbf{9.50}\times10^{-7}$	Helbert [this work]
C_3H_2	+	$h\nu$	$\longrightarrow$	C_3	+	H_2			$\mathit{1.9}\times10^{-6}$	Moses (2000, pers. comm.)
† C_3	+	$h\nu$	$\longrightarrow$	C_2	+	C			$\mathbf{2.00}\times10^{-5}$	Helbert [this work]
C_3	+	$h\nu$	$\longrightarrow$	C_2	+	C			$\mathit{1.00}\times10^{-4}$	(Huebner et al. 1992)
CH_4	+	$h\nu$	$\longrightarrow$	CH_3	+	H			2.64×10^{-7}	(Huebner et al. 1992)
CH_4	+	e	$\longrightarrow$	CH_3	+	H	+	e	9.43×10^{-10}	(Schmidt et al. 1988)
CH_4	+	$h\nu$	$\longrightarrow$	CH_2	+	H_2			5.44×10^{-6}	(Huebner et al. 1992)
CH_4	+	$h\nu$	$\longrightarrow$	CH_2	+	H	+	H	2.14×10^{-6}	(Huebner et al. 1992)
CH_4	+	$h\nu$	$\longrightarrow$	CH	+	H_2	+	H	6.39×10^{-7}	(Huebner et al. 1992)
CH_2	+	$h\nu$	$\longrightarrow$	CH	+	H			2.00×10^{-5}	(Huebner et al. 1992)
CH	+	$h\nu$	$\longrightarrow$	C	+	H			4.16×10^{-3}	(Huebner et al. 1992)
CH_3CN	+	$h\nu$	$\longrightarrow$	CH_3	+	CN			5.00×10^{-5}	(Huebner et al. 1992)
CH_3CN	+	e	$\longrightarrow$	CH_3	+	CN	+	e	3.80×10^{-8}	(Schmidt et al. 1988)